Optical Signal Routing Using Emission Packet Positioning of Semiconductor Heterostructure

H. Tsukamoto, *Senior Member, IEEE*, T. D. Boone, J. Han, *Senior Member, IEEE*, and J. M. Woodall, *Fellow, IEEE*

Abstract—We present a novel optical switching technique utilizing emission packet positioning of semiconductor heterostructure. A modulation-doped p-AlGaAs–GaAs heterostructure is employed to control spontaneous emission packet positioning with electric fields. Emission packets generated by optical input signals are brought over 150 μm with electric fields, so the output fibers can detect the emission intensity as signals. The first-order analysis indicates that the drift velocity of minority electrons in GaAs limits the detectable maximum data rate and nanoseconds timescale signal routing operation at 20 Gb/s is possible at an electron drift velocity of 2×10^7 cm/s.

Index Terms—Emission packet positioning, optical fiber communication, optical signal routing, semiconductor optical switch.

I. INTRODUCTION

SIGNAL routing performance of optical links limits the overall network speed and the flexibility of communication systems. In local area network computing such as short area grid computing, nanosecond timescale packet routing is desired when the system requires increased data exchange frequency between computers. In such a case, the transfer time for a unit packet of data needs to be shorter than a few microseconds to maintain minimized packet loss [1]. While recent research advances in microelectromechanical systems (MEMS) provide high flexibility of optical links in large-scale communication systems [2], [3], the speed of mechanical motion of MEMS-based switches (~1 ms) could limit the data exchange frequency between computers. Although wired-links are used for most parallel computing systems, high-speed optical routing devices are attractive for future computing networking systems because of their potentially higher data rate. We have previously reported on the application of spontaneous emission in direct bandgap semiconductors to high frequency optical modulators for short area optical networks, which indicated potentially higher bandwidth modulation of 10 Gb/s [4]. In this letter, we present a novel optical signal routing technique based on the two-dimensional positioning of emission packets in a semiconductor heterostructure and demonstrate the feasibility of multiple channel optical routing with electric fields.

II. DEVICE STRUCTURE AND OPERATION

A conceptual eight-channel optical routing device is shown in Fig. 1. The device consists of three kinds of layers: a p-type
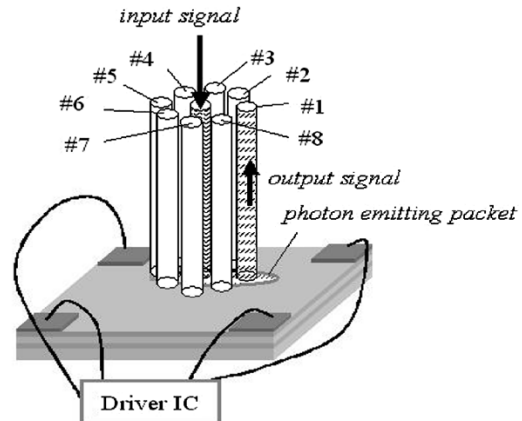
Fig. 1. A schematic illustration of an eight-channel semiconductor optical signal routing device.

modulation-doped AlGaAs potential barrier layer for minority electron confinement, an undoped GaAs channel layer sandwiched between the barrier layers, and a heavily doped p-type GaAs contact layer. An input-fiber is located at the center of the device, surrounded by output-fibers (#1–#8). Four contact pads on the device are positioned to generate the maximum electric field at any angle in the channel. The bandgap wavelength of an input signal is chosen to be larger than that of GaAs and smaller than that of AlGaAs barrier layers, so that the input signal effectively generates electron–hole packets in the channel. When a maximum electric field is formed in the Channel #1 region, the electron packet generated at the input fiber drifts toward Channel #1 and the hole packet drifts toward the opposite side (Channel #8). As high-density holes are provided in the channel layer by the modulation-doped barrier layers, radiative recombination dominates in the Channel #1 region where the electron packet drifts. As a result, the output Fiber #1 can detect the emission intensity as an output signal. Since the maximum electric field can be controlled with the combination bias at any angle, the angle of emission-packets can be used as signal routing channels. A sample structure was designed to confirm emission packet positioning with electric fields. All layers were grown on semi-insulating GaAs (001) substrate by molecular beam epitaxy (MBE) technique. A 50-nm-thick p-$Al_{0.9}Ga_{0.1}$As was grown after growing undoped GaAs buffer layer, followed by a 100-nm undoped GaAs channel layer. Subsequently, a 25-nm p-$Al_{0.9}Ga_{0.1}$As and a 50-nm p-$Al_{0.5}Ga_{0.5}$As were grown and the device structure was completed with a 10-nm p-GaAs growth on the top. The top GaAs layer and three AlGaAs layers were doped with beryllium atoms at 2×10^{19} cm^{-3}, which introduce free holes (~1×10^{18} cm^{-3}) into the channel layer. Because the channel
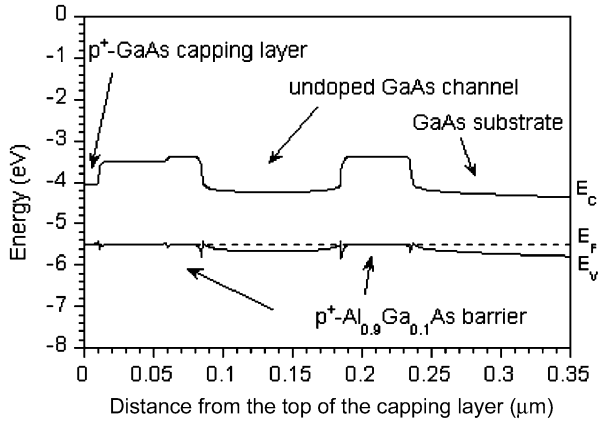
Fig. 2. A schematic band diagram of a sample structure designed with modulation-doped (Be) AlGaAs–GaAs heterostructure: p-GaAs(10 nm)/p-Al$_{0.5}$Ga$_{0.5}$As(50 nm)/p-Al$_{0.9}$Ga$_{0.1}$As(25 nm)/i-GaAs (100 nm)/p-Al$_{0.9}$Ga$_{0.1}$As(50 nm).

Fig. 3. Photos of photoemitting packets with different directions, indicating location of the four electrode pads with probes. (a) $+10$ V for the two upper pads, (b) $+10$ V for the two right side pads, (c) $+10$ V for the two bottom pads, (d) $+10$ V for the two left side pads. Due to the unequal distances between the four electrodes, the individual emissions have different lengths.

layer is an undoped GaAs layer, we expect that its minority electron mobility is around 2000 cm^2/V-s at room temperature. Four Ti–Au nonalloyed electrical contacts were formed on the top of the device structure. The band structure of the designed device is shown in Fig. 2.

III. EMISSION PACKET POSITIONING AND OUTPUT SIGNAL DETECTION

A photoluminescence measurement was performed to confirm that the spontaneous emission was generated in the channel layer of the device and the peak wavelength was 871 nm, corresponding to the bandgap of GaAs. A silicon charged coupled device camera was mounted on an optical microscope to image infrared (IR) emission from the device. With a two-channel function generator, individual output square shape biases (± 10 V) with distinguished phase were applied to the two pairs of electrodes of the device at a frequency of 1 Hz. A mode-lock pulse laser ($\lambda = 532$ nm, $\phi \sim 80$ μm, $P \sim 3$ mW, full-width at half-maximum (FWHM) ~ 50 ps, 76 MHz) was used to generate electron–hole packets in GaAs layer. Snapshots of IR emission packets at different angles are shown in Fig. 3. The electric probes and the electrodes are also indicated in Fig. 3(a). Bright emission packets are seen from the device at room temperature, indicating that the modulation-doped AlGaAs barriers provide high-density holes into the GaAs channel and that radiative recombination takes place. The emission packet immediately responds to the maximum electric field caused by the combination bias, as shown in Fig. 3(a), (b), (c), and (d). Due to rectangular arrangement of the four electrodes (horizontal distance > vertical distance), the emission length of horizontal direction is shorter than that of the vertical direction. When the bias signal is chosen to be sine wave with a slightly different phase, the emission packet smoothly turns either clockwise or counterclockwise, which shows feasibility of multiple channel optical signal routing. This characteristic would also make it simple to align output fibers on the device. The emission positioning can immediately respond to the maximum electric field caused by the biases. If a circuit of gigahertz frequency operation is used for biasing, the repositioning can occur in just a few nanoseconds.
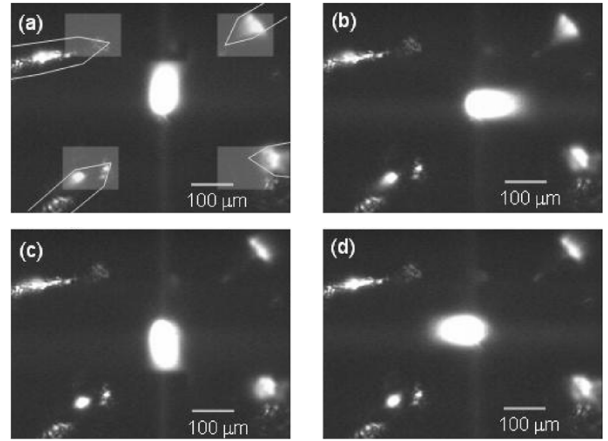
Output signals were detected through a single-mode fiber connected with a photon-counting measurement system. Pulses of the mode-lock laser were used as input signals. The electric clock pulses of the mode-lock laser were led to the photon counting system as reference signals. A mesa stripe sample was used for the experiment. The laser spot diameter ϕ of the input signals was $\phi \sim 80$ μm and the output fiber (single mode) was set at 80 μm apart from the center of the original laser spot, so that there was no signal detected when the electric field is zero. The emission spots with the electric field and under a bias of 20 V ($E \sim 0.9$ kV/cm) are shown in Fig. 4(a) and (b), respectively. It is seen that the emission packet extends about 200 μm from the original spot, as shown in Fig. 4(b). The maximum applied bias (20 V) is limited due to imperfect ohmic contacts of this device. The length of the emission packets is long enough to put a single or multimode optical fiber tip as signal output probes. The bright packets look like continuous emission in Fig. 4, however, actual emission turns ON and OFF according to the laser pulse duration, decaying as a function of the radiative recombination lifetime of the material.

The detected signals through the output fiber are shown on the bottom of Fig. 4. It is seen that the input signals are successfully delivered to the output fiber and detected as output signals. Due to the limitation of timescale window of the measurement system, only half of the second pulse is shown and the rest of the pulse is indicated with broken lines. From the pulsewidth detected, we can estimate the maximum data rate of this device. Since the present experiment is equivalent to a time-of-flight measurement of minority carriers under electric fields, the first report by Haynes and Shockley [5], the distribution of the minority carrier (electron in the present case) as a function of the distance x and time t is written in terms of carrier diffusion, drift, and recombination lifetime [6]–[8], as follows:

$$n(x,t) = \frac{N_e}{\sqrt{4\pi Dt}} \exp\left(\frac{-(x-vt)^2}{4Dt}\right) \exp(-t/\tau_r) \qquad (1)$$

where N_e is the number of electrons generated per unit area, D is a diffusion constant of minority electrons, v is the drift
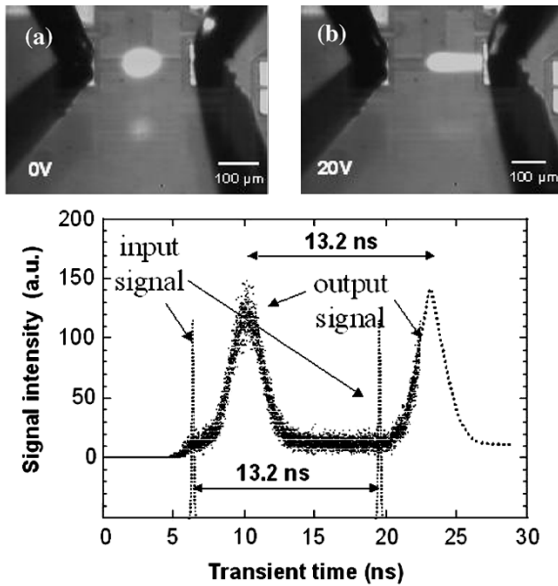
Fig. 4. Typical pulse shape from the device measured with a signal output fiber. The duration of pulse-to-pulse is approximately 13.2 ns. Due to the limitation of time window of the equipment, only half of the second pulse is seen and the rest is indicated as the dashed line. The mode-locked laser pulses are indicated in the figure as a reference.

velocity, t is time, and τ_r is a radiative recombination lifetime, respectively. The equation indicates that the minority electron packet drifts with emitting photons as a function of time $\exp(-t/\tau_r)$. This means that the maximum distance of an electron packet is limited by recombination lifetime. When the lifetime is extremely short, the distance becomes shorter and it will eventually become too short to use output fibers for signal detection. Thus, there is an optimum condition for heterostructure design. The approximate time delay t_d of the signal is read to be ∼4.5 ns from Fig. 4. By using $t_d = d/\mu E = d/v$ for a distance d (∼80 μm) between the input and output fibers and electric field $E \sim 0.9$ kV/cm, the electron mobility and the drift velocity obtained are $\mu = 1975$ cm^2/V·s and $v \sim 1.78 \times 10^6$ cm/s, respectively. At the observation point, the total signal width depends on the time duration of emission packet sweeping across the diameter of the output optical fiber ($\Phi = 5$ μm). Since the total detectable time is determined by the input laser spot size ($\phi \sim 80$ μm) and the core diameter of the output fiber, the approximate pulsewidth t_p is obtained by $t_p \sim (\Phi + \phi)/v$. In the present experiment, we can read the total pulsewidth being $t_p \sim 5$ ns from Fig. 4, which is consistent with our calculation. The equation also indicates that the output signals can be degraded with the minority electron diffusion in the channel during lateral drift. The diffusion length $(Dt)^{1/2}$ is roughly estimated to be 5 μm assuming $D \sim 60$ cm^2/s and $t = 4.5$ ns ($= t_d$). This can be a limitation for the maximum data rate of the present device structure. However, by improving the ohmic contact of the electrodes and narrowing the input beam diameter, it would be possible to obtain 50-ps output signal pulses, roughly corresponding to a data rate of 20 Gb/s, for $\phi \sim 5$ μm, $\Phi = 5\mu$m and an electron drift velocity of 2×10^7 cm/s. Further improvement of the data rate would

be possible by choosing materials with higher electron drift velocities. To confirm this hypothesis, thorough analysis of the output pulse shape and drift velocity is under investigation.

As discussed above, the present technique has the potential advantages of fast operation, easy-fiber alignment, and relatively simple device structure, whereas there is an essential loss in the present technique due to the utilization of spontaneous emission. Since electron-holes generated by input signals equally emit photons both sides the front and bottom of the device, half of the signal intensity is ideally the maximum as the output signal. Additionally, an extra loss is obtained by calculating the area of the output fiber core that can detect the emission signal. If the core area is much smaller than the total emission area, the detecting signal level with the output fiber could be seriously low. For the present experiment, the available output power by the output fiber is roughly estimated to be 0.15 μW, taking into account the reflection at the sample surface and absorption coefficient of the active layer. To avoid such a condition, the input beam spot size needs to be a few micron diameters and high-sensitive photon detectors with high-speed operation would need to be coupled to the end of the output fibers.

IV. SUMMARY

We have presented a novel optical signal routing technique based on two-dimensional emission packet positioning in a semiconductor heterostructure and demonstrate feasibility of multiple channel optical routing with electric fields. The potential issues were also discussed.

ACKNOWLEDGMENT

REFERENCES

[1] M. Mathis, J. Semke, J. Mahdavi, and T. Ott, "The macroscopic behavior of the TCP congestion avoidance algorithm," *ACM Comput. Commun. Rev.*, vol. 27, pp. 67–82, Jul. 1997.

[2] R. M. Boysel, "A 1920 × 1080 element deformable mirror device for high-definition displays,," *IEEE Trans. Electron Devices*, vol. 38, no. 12, p. 2715, Dec. 1991.

[3] L. Y. Lin, E. L. Goldstein, and R. W. Tkach, "Free-space micromachined optical switches with submillisecond switching time for large-scale optical crossconnects," *IEEE Photon. Technol. Lett.*, vol. 10, no. 4, pp. 525–527, Apr. 1998.

[4] T. D. Boone, H. Tsukamoto, and J. M. Woodall, "Intensity and spatial modulation of spontaneous emission in GaAs by field aperture selecting transport," *Appl. Phys. Lett.*, vol. 82, pp. 3197–3199, May 2003.

[5] J. R. Haynes and W. Shockley, "The mobility and life of injected holes and electrons in Germanium," *Phys. Rev.*, vol. 81, pp. 835–843, Mar. 1951.

[6] R. A. Hoepfel, P. A. Wolff, and A. C. Gossard, "Negative absolute mobility of minority electrons in GaAs quantum wells," *Phys. Rev. Lett.*, vol. 56, pp. 2736–2739, Jun. 1986.

[7] K. Kaede, Y. Arakawa, P. Derry, J. Pasiaski, and A. Yariv, "High-speed GaAs/AlGaAs photoconductive detector using a p-modulation-doped multiquantum well structure," *Appl. Phys. Lett.*, vol. 43, pp. 1096–1097, Apr. 1986.

[8] E. Inuzaka, K. Ishida, and Y. Mizuhima, "Observation of minority-carrier drift by infrared radiation," *IEEE Trans. Electron Devices*, vol. 37, no. 7, pp. 1532–1533, Jun. 1990.